2023 EAGE ANNUAL
84TH CONFERENCE & EXHIBITION
VIENNA | AUSTRIA

3D geomechanical modelling of induced seismicity including intersecting faults and reservoir compartments

J. Ruan[1], R. Ghose[1], W. Mulder[2,1]

[1] Delft University of Technology; [2] Shell Global Solutions International BV

Summary

To investigate the physical processes behind induced seismicities due to, for example, production of hydrocarbons from a reservoir, most of the earlier studies performed geomechanical simulations on a simple reservoir geometry. The effect of fluid depletion is, in general, simulated for such a simple geometry. Neglecting the contribution of realistic 3-D reservoir geometries can lead to a wrong estimation of the incremental stress field. A reliable estimate of the induced stress field is key to producing meaningful simulation results. We perform geomechanical simulations on a simple fault model as well as a more realistic model based on the known geological structures at the earthquake source-region in Zeerijp region, the Netherlands. Our results demonstrate that the angle of the fault intersection affects the incremental stress field, including the effective normal stress, the shear stress, and hence, the Coulomb stress and the SCU value. Our results also show a shift in the rupture pattern and the location of the maximum slip on the fault plane. We conclude that, to properly evaluate the effects of production activities and to simulate precisely the in-situ stress field and the induced seismicity, the incorporation of a realistic reservoir structure in modelling is essential.

3D geomechanical modelling of induced seismicity including intersecting faults and reservoir compartments

Introduction

Production activities affecting the pore pressure in an underground reservoir can cause induced earthquakes. Induced seismicity has been studied extensively for the Groningen gas field in the Netherlands. Kühn et al. (2022) reviewed earthquake source models for the Groningen gas field based on various approaches, including physical models, while trying to understand the physical relation between gas extraction and the induced earthquakes. Geomechanical simulation considering poroelasticity is commonly used to simulate induced seismicity from a depleted reservoir.

The pore-pressure variation in the reservoir will induce a poroelastic stress, which, according to the Mohr-Coulomb theory, will promote the failure of fractures in the reservoir. Apart from the poroelastic stress, the differential compaction due to faulting with non-zero offsets can contribute to incremental stresses, including shear stress and normal stress. This effect has been observed in numerical modelling by Buijze et al. (2019) and Van den Bogert (2018). The analytical expression for such an effect for a homogeneous medium has been derived by Jansen and Meulenbroek (2022).

Most geomechanical simulations assume a simple 2-D or 3-D model, neglecting the contribution of a realistic reservoir geometry. This assumption could lead to an underestimated incremental stress field. In this study, we perform geomechanical simulations considering a realistic reservoir structure for the Zeerijp region of Groningen. We have chosen the research area following the inversion results of the 2018 Zeerijp M_L 3.4 event by Dost et al. (2020).

We design at first a set of representative, simple geological models for the earthquake source-region at Zeerijp. The representative models contain the major features of the reservoir structure, which are the fault intersection and the resulting three compartments. The simulation includes quasi-static and dynamic modelling of the incremental stress field due to reservoir depletion and the resulting fault reactivation when the fault becomes unstable. Then we simulate induced seismicity using the realistic reservoir geometry in the Zeerijp region.

Method

In this study, we simulate induced seismicity using the open-source package Defmod developed by Meng (2017). Defmod simulates induced seismicity in two phases. The simulation is first conducted in a quasi-static manner, where linear poroelasticity is considered to simulate the long-term effect of gas extraction. The governing equation can be described as follows:

$$\mathbf{K}_n\mathbf{U}_n = \mathbf{F}_n \quad \text{(absolute)}, \qquad \mathbf{K}_n\Delta\mathbf{U}_n = \Delta\mathbf{F}_n \quad \text{(incremental)}, \tag{1}$$

where $\mathbf{K}$ is the system stiffness matrix, $\mathbf{U}$ is the solution vector and $\mathbf{F}$ the nodal force, including fluid source. The subscript n is the time index. The solution $\Delta\mathbf{U}_n$ includes the nodal displacement and the pressure, where $\Delta\mathbf{U}_n = \begin{bmatrix} \Delta\mathbf{u}_n \\ \Delta\mathbf{p}_n \end{bmatrix}$.

The stiffness matrix $\mathbf{K}_n$ and the right-hand-side vector $\mathbf{F}_n$ have the following form:

$$(\mathbf{K}_n, \Delta\mathbf{F}_n) = \left(\begin{bmatrix} \mathbf{K}_e & \mathbf{H} \\ -\mathbf{H}^T & \Delta t\mathbf{K}_c + \mathbf{S}_p \end{bmatrix}, \begin{bmatrix} \Delta\mathbf{f}_n \\ \mathbf{q}_n - \Delta t\mathbf{K}_c\mathbf{p}_{n-1} \end{bmatrix} \right), \tag{2}$$

where $\mathbf{K}_e$ is the elastic stiffness matrix and depends on the elastic constants of the solid. $\mathbf{K}_c$ is the fluid stiffness matrix, depending on the fluid flow conductivity. $\mathbf{H}$ is the coupling matrix, depending on Biot's coefficient, responsible for coupling the displacement to pressure fields. $\mathbf{S}_p$ is the storage matrix, depending on solid compressibility, fluid compressibility and porosity. The combination of the system is

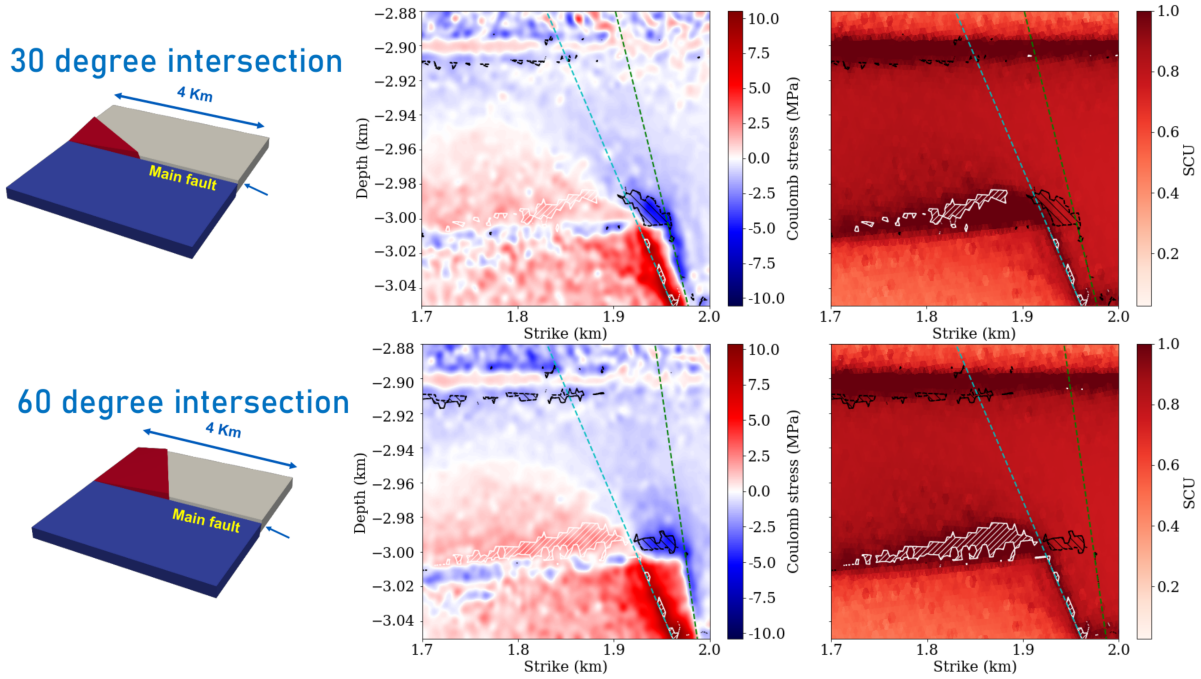

Figure 1 *Reservoir geometry in the representative models and the comparisons on the induced stress field at the main fault from different intersection angle, showing the incremental Coulomb stress difference (in the middle) after 18 MPa depletion and the difference on the SCU value (on the right) when the earthquake occurs compared with the model with a 30° intersection angle. Top: comparison between models with 30° and 45° intersections. Bottom: comparison between models with 30° and 60° intersections. The blue dashed line denotes the intersection for the model with a 30° intersection. The white dashed area marks the additional critical area in the model with 30° intersection compared with 40° and 60° intersection, and the black dash area the reduced critical area for the model with the 30° intersection.*

accomplished by the coupling matrix **H**. The solution of this system provides the equilibrium between the displacement and the pressure fields.

When the fault reaches a critical state, where the shear stress exceeds the fault strength, the fault is reactivated. Ground acceleration occurs when the seismic waves reaches the surface. In this phase, therefore, the modelling has to switch to the elastodynamic equations,

$$\mathbf{M\ddot{u}} + \mathbf{C\dot{u}} + \mathbf{Ku} = \mathbf{f}, \tag{3}$$

where **M** is the mass matrix, $\mathbf{C} = \alpha_\eta \mathbf{M} + \beta_\eta \mathbf{K}$ the damping matrix, and α and β are the Rayleigh damping coefficients. In Defmod, the fault constraints are implemented via the Lagrange Multiplier capping method. For a model containing a fault, each node except the edge nodes of the fault is split into a node-pair sharing the same coordinates. The constraints limit the displacement and pressure of the node-pairs. Equation 3 describes the displacement on nodes without constraints. For the simulation of a fault failure, a constrained dynamic solution is achieved by the forward incremental Lagrange Multiplier method. For details on fault constraints, see Meng (2017).

Representative models for reservoir structures in the Zeerijp region, Groningen

To understand better the effects of the reservoir geometry in the Zeerijp region, we have developed a set of representative models that focus on the major features in the source region, including varying fault offsets, fault intersection angles, and the shape of the resulting reservoir compartments. We investigate the effects of these major features on the induced stress field due to reservoir depletion and fault reactivation.

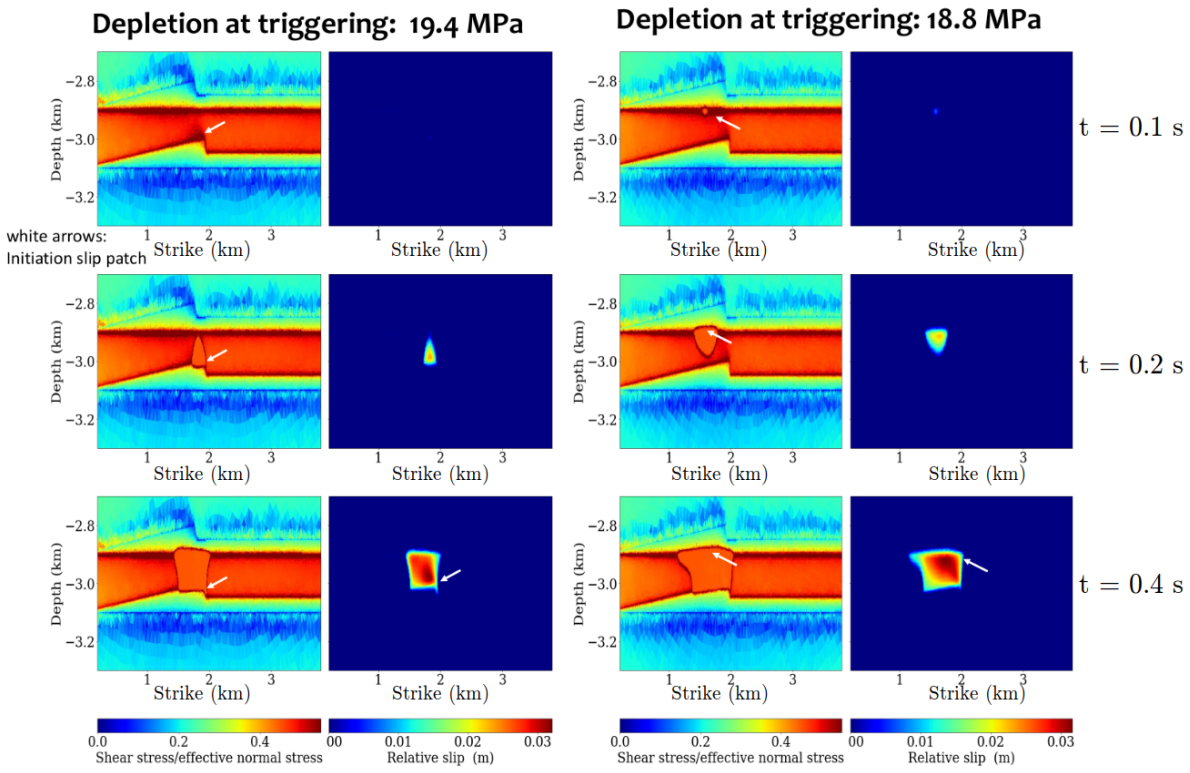

Figure 2 *Results of dynamic simulation of seismic events showing the stress field and the displacement. Left: the model with 30° intersection angle. Right: the model with 60° intersection angle.*

Next, we include a secondary fault inside the model—intersecting the main fault in the middle to form reservoir compartments. The secondary fault, a vertical planar fault with a dip of 90°, has an azimuth based on the intersection angles with the main fault, which are chosen to be 60°, 45°, or 30°. The main fault has a dip of 66° and cuts through the entire model, while the secondary fault ends at the intersection with the main fault. Both faults have the same offset of 50 m on the reservoir, where the main fault has varying offsets and the secondary fault has a constant offset. The main fault first offsets the reservoir, then the secondary fault, resulting in a 3-compartment setup. The intersection angle controls the shape of the compartments and, thus, the effects of reservoir geometry on the induced stress field from reservoir depletion. The simulation evaluates only the stress state of the main fault, as it corresponds to the seismogenic fault from the 2018 Zeerijp M_L 3.4 event, according to Wentinck (2018).

The models are initialized with the gravity-based initial stress and hydrostatic pressure. We applied roller boundary conditions at the side walls and at the bottom to simulate a laterally extended reservoir. After the initialization, we applied uniform depletion in the reservoir to simulate pore pressure change due to gas extraction. Linear-weakening friction is considered for the main fault in the models. By quasi-static simulation, we model the induced stress field due to reservoir depletion until the main fault reaches the critical state where the shear capacity utilization $SCU > 1$, SCU being the ratio between the shear stress and the maximum friction. Then, we simulate the fault reactivation dynamically, which could be either seismic or aseismic.

Results

Figure 1 shows the difference in incremental Coulomb stress at the main fault between the models with 30° and 60° intersection angles, after 18 MPa reservoir depletion. Note that intersection angle affects the location of the reservoir compartment, thus also affecting strongly the distribution of pressure depletion on the main fault. The lower half of the reservoir juxtaposition shows a positive value, indicating the promotion of slip in this area. The maximum value is observed at the fault intersection. However, this is due to the change in the location of the secondary fault. The white dashed area in the SCU value

indicates that a sharper intersection angle can significantly increase the slip patch in the lower half of the reservoir juxtaposition.

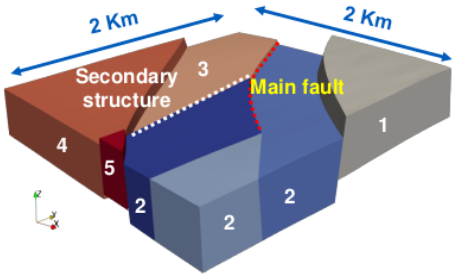

Figure 3 *The reservoir geometry for the realistic Zeerijp model. The numbers denote the reservoir compartments seperated by the fault system.*

The depletion values required for a seismic event for models with 30°, 45°, or 60° intersection angles between main fault and secondary fault are 19.4 MPa, 19.25 MPa and 18.8 MPa, respectively. Figure 2 shows the results of dynamic simulation of a depletion-induced earthquake for models with 30° and 60° intersection angles. The result for the model with 30° intersection angle shows an initial slip patch at the bottom of the reservoir juxtaposition interval close to the intersection line. The slip patch expands from the bottom to the top of the juxtaposition. The slip patch also expands in the strike directions and is then arrested. The result for the model with 60° intersection angle shows, on the other hand, that the initial seismic slip patch occurs at the top of the reservoir juxtaposition interval close to the intersection line. In this case, the initial slip patch expands in both dip and strike directions, and is then arrested at a location which is close to that for the model with 30° intersection angle. The maximum slip locations are the same as the location of the initial slip patch. The realistic model (Figure 3) has an event magnitude of M_L3.0, reactivated at a depletion value of 26 MPa, similar to parameters from the Zeerijp 2018 M_L3.4 event, by Wentinck (2018). The rupture location is also closed to the inverted hypocenter by Dost et al. (2020).

Discussion and conclusions

We have performed quasi-static and dynamic simulations of induced seismicity, considering realistic reservoir structure at Zeerijp in the Groningen gas field. The results from representative models show that the intersection of two normal faults and the angle of their intersection significantly affect the induced stress field. A sharper intersection angle increases the incremental Coulomb stress at the lower half of the reservoir juxtaposition. When the intersection angle changes from 60° to 30°, the location of the initial slip patch changes from the top to the bottom of the reservoir juxtaposition, close to the intersection line. The rupture pattern also changes according to the location of the initial slip patch. The location of the area of maximum slip is the same as that of the initial slip patch. Clearly, the reservoir geometry and the intersection of faults significantly affect the process of reactivation of a preexisting fault in terms of incremental stress field due to reservoir depletion and the rupture pattern. Our simulation using realistic reservoir geometry in the Zeerijp region also shows comparable results from the inversion of the Zeerijp 2018 M_L3.4 event. Therefore, In order to simulate induced seismicity in a specific region, it is necessary to consider realistic reservoir structure at the source region of an earthquake.

References

Van den Bogert, P. [2018] Depletion-induced fault slip and seismic rupture-2D Geomechanical models for the Groningen field, The Netherlands. *Assen: Nederlandse Aardolie Maatschappij BV*.

Buijze, L., Van den Bogert, P., Wassing, B. and Orlic, B. [2019] Nucleation and arrest of dynamic rupture induced by reservoir depletion. *Journal of Geophysical Research: Solid Earth*, **124**(4), 3620–3645.

Dost, B., van Stiphout, A., Kühn, D., Kortekaas, M., Ruigrok, E. and Heimann, S. [2020] Probabilistic moment tensor inversion for hydrocarbon-induced seismicity in the Groningen gas field, the Netherlands, part 2: Application. *Bulletin of the Seismological Society of America*, **110**(5), 2112–2123.

Jansen, J.D. and Meulenbroek, B. [2022] Induced aseismic slip and the onset of seismicity in displaced faults. *Netherlands Journal of Geosciences*, **101**.

Kühn, D., Hainzl, S., Dahm, T., Richter, G. and Rodriguez, I.V. [2022] A review of source models to further the understanding of the seismicity of the Groningen field. *Netherlands Journal of Geosciences*, **101**.

Meng, C. [2017] Benchmarking Defmod, an open source FEM code for modeling episodic fault rupture. *Computers & Geosciences*, **100**, 10–26.

Wentinck, H. [2018] Dynamic modelling of large tremors in the Groningen field using extended seismic sources. *Assen: Nederlandse Aardolie Maatschappij BV*.